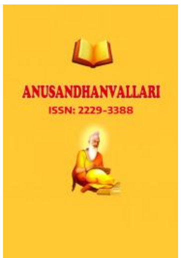


Anusandhanvallari
Vol 2019, No.1
December 2019
ISSN 2229-3388

# Investigation and Optimization of Process Parameters in Ultrasonic Metal Welding for Achieving Quality Welds: A Taguchi–RSM–GA Approach with Thermal-FEA Validation

**Ramesh Babu Yeluri[1], Dr. P. Manoj Kumar[2] (Supervisor), Dr. Prashant S. Kadu[3] (Co-Supervisor)**

[1,2]Department of Mechanical Engineering Sri Satya Sai University of Technology & Medical Sciences, Sehore, Madhya Pradesh, India

[3]Principal, Abha-Gaikwad Patil College of Engineering, Nagpur

**Abstract:** Ultrasonic metal welding (USMW) is a solid-state joining process in which high-frequency, low-amplitude relative motion applied under moderate normal pressure disperses surface oxides and produces intimate metal-to-metal contact without bulk melting. Because weld quality is governed by a narrow, interacting band of process parameters, this study presents an integrated framework for investigating and optimizing welding pressure, weld time and vibration amplitude for aluminium, copper and copper–brass lap joints. The work is organized in three phases: preliminary trials to bound the usable parameter range; a Design-of-Experiments phase combining the Taguchi orthogonal-array method (with ANOVA-based percentage contribution) and Response Surface Methodology (RSM) using a Face-Centred Central Composite Design, coupled with a Genetic Algorithm (GA) that treats the RSM regression model as its fitness function; and a thermal-field phase in which interface temperatures measured by thermocouple and infrared thermography are compared against Finite Difference Method (FDM) and Finite Element Analysis (FEA) predictions. For Cu–Cu welding, weld pressure, weld time and amplitude were found to contribute approximately 20%, 30% and 9% respectively to the variation in weld strength, with the pressure–time and pressure–amplitude interactions contributing a further 23% and 10%. Maximum weld strength was obtained near 3 bar pressure, 3 s weld time and 57 µm amplitude, while minimum strength scatter occurred near 3 bar, 2.5 s and 42.5 µm. RSM–GA optimization for Al and Cu/Cu–brass joints produced second-order regression models whose GA-optimized predictions agreed closely with experimental weld-bead density and resistance. FEA and FDM temperature-field predictions matched thermocouple and thermal-imaging measurements within acceptable limits, confirming that interface temperature rises with amplitude and weld time up to a threshold before joint degradation sets in. The results provide a validated, statistically grounded parameter-selection methodology that industry can use to replace trial-and-error tuning of USMW processes.

**Keywords:** Ultrasonic Metal Welding; Taguchi Method; Response Surface Methodology; Genetic Algorithm; ANOVA; Finite Element Analysis; Weld Strength Optimization

## 1. Introduction

Ultrasonic metal welding (USMW) joins similar or dissimilar metallic work-pieces using high-frequency vibrations applied in the plane of the interface under moderate clamping pressure. The resulting relative shearing motion between the mating surfaces disrupts surface oxide films and asperities, promoting localized plastic deformation and solid-state bonding without melting the parent metal. Because the process does not rely on fusion, it consumes markedly less energy than resistance or arc welding, produces minimal heat-affected zones, and is well suited to joining thin sheets, foils and dissimilar metal combinations — for example aluminium-to-copper connections widely used in electrical, battery and automotive wiring assemblies.

Despite these advantages, the industrial application of USMW has historically been limited by an incomplete understanding of how the governing process parameters — weld pressure (clamping force), weld time and vibration amplitude — interact to determine weld strength, weld-bead density and interface temperature. Many manufacturers still rely on trial-and-error parameter selection, which increases cycle time, scrap rates and cost. This paper reports a structured investigation that combines classical Design-of-Experiments techniques with soft-computing optimization and numerical thermal modelling to establish a defensible, repeatable basis for USMW parameter selection.

The industrial relevance of this problem has grown alongside the shift toward lightweight, multi-material assemblies. Aluminium-to-copper USMW joints are now central to electric-vehicle battery-tab and busbar connections, where low contact resistance, high joint consistency and minimal heat input are simultaneously required; to consumer electronics and communication-device assembly, where miniaturized components cannot tolerate the thermal distortion associated with fusion welding; and to general electrical wiring harnesses, where dissimilar-metal joints must resist vibration and thermal cycling over the product lifetime. In each of these applications, the cost of an under-optimized weld schedule is not merely scrap material but downstream reliability risk, since a marginally bonded joint may pass an initial visual or pull-test inspection yet fail prematurely in service. This risk is amplified by the fact that, as shown in Section 5, the parameter combination that maximizes average weld strength is not always the combination that minimizes strength variability — a distinction that trial-and-error tuning is poorly equipped to reveal, but that a structured DOE and ANOVA-based approach makes explicit.

Against this backdrop, the specific contribution of the present work is to combine three techniques — each individually well established in the literature (Ross, 2005; Elangovan et al., 2012; Elangovan, Semeer, & Prakasan, 2009) — into a single validated pipeline applied consistently across three material systems (Al–Al, Cu–Cu and Cu–brass) and two weld geometries (spot and seam), with mechanical-strength optimization cross-checked against an independent thermal-field model rather than treated as a separate, unconnected study.

## 2. Literature Background

Prior work on USMW and related solid-state joining processes has approached parameter optimization from several angles, spanning vibration-transmission mechanics, statistical design of experiments, soft-computing optimization and numerical/thermal modelling. This section reviews each of these strands and positions the present study relative to them.

### 2.1 Vibration Transmission, Horn Design and Bonding Mechanism

Li, Tan, Lei and Jue (2004) examined the transducer, vibration-transmission path and coupling characteristics of USMW equipment, showing that ultrasonic vibration displacement, velocity and energy density increase as the cross-section of the transducer decreases, and that controlling frequency, displacement and phase in a longitudinal–torsional composite vibration system improves the resulting joint microstructure and mechanical/electrical performance. Kim, Sung, Kim and Park (2010) carried out vibration analysis of the ultrasonic welding horn to optimize its modal behaviour for a given application, reinforcing the finding that horn geometry directly governs the amplitude and uniformity of energy delivered to the weld interface. deVries (2004) and Graff (2005) provide foundational treatments of the mechanics and mechanisms of ultrasonic metal welding, establishing that bonding proceeds through progressive shearing, oxide dispersal and localized plastic deformation rather than bulk melting, while Bloss and Graff (2009) extended the process envelope to advanced alloys including stainless steel, titanium and nickel-based superalloys.

### 2.2 Taguchi and Statistical DOE Approaches

Taguchi's design-of-experiments methodology, using orthogonal arrays and signal-to-noise ratio analysis, has been widely applied to welding-process optimization. Tarng, Yang and Juang (2000) combined fuzzy logic with the Taguchi method to simultaneously optimize multiple submerged-arc weld-bead characteristics, while Tarng and Yang (1998) applied the Taguchi method to gas tungsten arc weld-bead geometry optimization, demonstrating that the approach gives a systematic and economical procedure for searching the process window. Datta, Bandyopadhyay and Pal (2008) used a Grey-based Taguchi method to optimize submerged-arc bead-on-plate geometry with multiple, sometimes conflicting, quality characteristics. Pradeep Kumar and Prakasan (2012) applied a full-factorial DOE with ANOVA specifically to USMW of copper wire to copper sheet using a lateral-drive system, varying weld pressure, amplitude and weld time — the same three factors adopted in the present study. Pop-Calimanu and Fleser (2012) likewise identified weld pressure and weld time as the dominant factors governing aluminium-composite ultrasonic weld strength. Ross (2005) remains a standard reference for the underlying Taguchi quality-engineering methodology used here.

### 2.3 Response Surface Methodology and Genetic Algorithm Optimization

RSM has been used across a range of manufacturing processes to fit predictive second-order models: Gunaraj and Murugan (1999) applied RSM to predict submerged-arc weld-bead quality in pipe welding; Onwubolu and Kumar (2006) applied it to CNC drilling; and Habib (2009) applied it to electrical-discharge-machining parameter selection. Within USMW specifically, Elangovan, Anand and Prakasan (2012) developed an RSM model coupled with a Genetic Algorithm to optimize USMW parameters, validating GA-predicted optima against experimental measurements — the same RSM–GA coupling strategy adopted in this study. Elangovan, Prakasan and Jaiganesh (2010) extended this approach to copper-to-brass ultrasonic joints using a face-centred central composite design, reporting that weld strength is sensitive to pressure, weld time and amplitude in a manner consistent with the results obtained here for Cu/Cu–brass joints. Meran (2006) used a genetic algorithm to predict optimal welding parameters for joined brass plates, and Canyurt, Kim and Lee (2008) applied a GA to estimate laser hybrid weld-joint strength, both confirming that population-based stochastic search outperforms deterministic hill-climbing for multi-modal weld-strength response surfaces.

### 2.4 Thermal and Finite Element Modelling

Elangovan, Semeer and Prakasan (2009) developed an FEA-based model capable of predicting interface temperature and stress distribution during USMW as functions of material thickness, clamping force, weld time and the coefficient of friction, finding that clamping force plays a dominant role in the deformation area and hence the force developed at the weld interface — a result mirrored in the present thermal-field analysis. Watanabe, Sakuyama and Yanagisawa (2009) modelled and measured USMW of dissimilar mild-steel-to-Al–Mg-alloy sheet joints, providing comparative interface-temperature data used to benchmark the present FDM/FEA results. Hiraishi and Watanabe (2003) investigated surface-treatment effects (alcohol adhesion) on USMW weld strength for Al–Mg alloy, underscoring the sensitivity of bond quality to interfacial surface condition — consistent with the oxide-dispersal mechanism central to this work.

### 2.5 Dissimilar-Metal Joining, Microstructure and Process Monitoring

Flood (1997) and Ganesh and Praba Rajathi (2013) reported early practical demonstrations of ultrasonic joining of copper to aluminium, quantifying the pressure, time and power ranges over which acceptable bonding occurs and noting the process's relevance to electrical and automotive wiring applications. Jeng and Horng (2001) used a micro-contact model to explain that contact temperature governs bond formation in the initial stage of ultrasonic wire bonding while surface roughness becomes the dominant factor in later stages — a two-stage bonding mechanism consistent with the weld-time thresholds identified in Sections 5.1–5.2 of this paper. Acarer, Demir and Findik (2004) examined explosively welded steel/steel joints, showing that post-weld heat treatment and interface morphology strongly influence bond strength, a finding echoed qualitatively in the amplitude–strength trade-off identified for USMW. Annoni and Carboni (2011) characterised the static mechanical behaviour of ultrasonically welded AA6022-T4 lap joints, and process-monitoring studies using electrical/vibration signatures (Wen & Iwamura, 2008; Hsiao, Xu, Lin, & Tsai, 2008) illustrate complementary soft-computing approaches — fuzzy control and neural-network-based robustness design — that could, in future, be combined with the Taguchi–RSM–GA pipeline used here.

Across this body of work, welding pressure, weld time and vibration amplitude recur consistently as the three parameters with the greatest influence on USMW bond quality, and FEA is repeatedly validated as an effective tool for predicting interface temperature and stress. However, a unified pipeline that combines Taguchi/ANOVA screening, RSM–GA optimization and independent FDM/FEA thermal validation across multiple material systems (Al, Cu and Cu–brass) — the approach adopted in this paper — has not been comprehensively reported in a single study, motivating the integrated methodology described in Section 4.

**3. Problem Definition and Objectives**

Inconsistent weld quality and durability in USMW are traced principally to poorly chosen combinations of weld pressure, weld time and vibration amplitude, compounded by a lack of validated thermal models linking interface temperature to bond formation. This creates a need for a systematic, economically viable procedure for selecting USMW process parameters that can be adopted directly by industry. The specific objectives of this study are:

- Characterize the achievable range of welding pressure, weld time and vibration amplitude for aluminium, copper and brass work-pieces through preliminary trials.
- Design and execute Taguchi orthogonal-array experiments (with ANOVA) to identify the parameter combination that maximizes weld strength and minimizes strength variability for Cu–Cu joints.
- Develop second-order RSM regression models (Face-Centred Central Composite Design) relating weld pressure, weld time and amplitude to weld-bead density/strength for Al and Cu/Cu–brass joints.
- Couple the RSM regression models with a Genetic Algorithm to obtain globally optimized parameter sets, and validate GA-predicted optima against experimental results.
- Measure interface temperature during welding using thermocouples and infrared thermography, and model the temperature field using the Finite Difference Method and Finite Element Analysis.
- Compare experimental, FDM and FEA temperature results, and establish the relationship between interface temperature and weld resistance.

**4. Materials and Methodology**

The study was executed in three phases, summarized in Figure 1 and described below.

Figure 1. Three-phase research methodology: (I) preliminary parameter bounding, (II) Taguchi/RSM/GA optimization, (III) thermal-field modelling and validation.

**4.1 Phase 1 — Preliminary Trials**

Aluminium, copper and brass foil specimens were prepared as lap joints in accordance with ASTM D1002-01 (ASME International, 2005), the standard test method for apparent shear strength of single-lap-joint adhesively/mechanically bonded metal specimens under tension loading. Specimens cleaned along a 6 mm bond-line were mounted between the welding horn and anvil on a lateral-drive ultrasonic spot-welding rig, consistent with the lateral-drive configuration described by Li et al. (2004) and adopted by Pradeep Kumar and Prakasan (2012) for copper wire-to-sheet USMW. Trial welds were made across a wide range of pressure, time and amplitude settings to identify the lower bound (below which no bonding occurs) and the upper bound (above which the sonotrode sticks to the specimen) for each material. These bounds defined the factor ranges used in the Phase 2 experimental designs, and are broadly consistent with the pressure and amplitude windows reported for comparable Al–Cu and Cu–brass systems by Ganesh and Praba Rajathi (2013) and Elangovan et al. (2010).

Post-weld strength evaluation used a computerized universal testing machine (UTM) of the type used in comparable USMW studies (Pradeep Kumar & Prakasan, 2012), with specifications summarized in Table A.

| UTM Specification | Value |
|---|---|
| Maximum capacity | 10 kN |
| Least count (displacement) | 0.1 mm |
| Load accuracy | ±1% of indicated load, 4–100% of load-cell capacity |
| Grip separation range | 25–750 mm |
| Straining rate range | 1–100 mm/min |
| Power supply | Single-phase, 220 V, 50 Hz AC |

**Table A. Representative universal testing machine (UTM) specifications used for post-weld tensile/shear strength evaluation.**

**4.2 Phase 2 — Design of Experiments**

Two complementary DOE strategies were used, following established practice in the welding-optimization literature (Ross, 2005; Tarng & Yang, 1998; Gunaraj & Murugan, 1999). First, a Taguchi orthogonal-array design was used to screen the Cu–Cu welding parameters (pressure, weld time, amplitude) at three levels each, with weld strength recorded via a computerized tensile testing machine and analyzed using signal-to-noise ratios and ANOVA in MINITAB. Second, a Face-Centred Central Composite Design (CCF, a non-rotatable RSM architecture) — the same architecture used by Elangovan et al. (2010, 2012) for copper-to-brass USMW optimization — was used for Al and Cu/Cu–brass joints to fit second-order regression models predicting weld-bead density and weld resistance as functions of the same three factors.

**Table 1. Representative process-parameter levels used in the Taguchi/RSM experimental design.**

| Parameter | Symbol | Low | Mid | High |
|---|---|---|---|---|
| Welding pressure (bar) | P | 1.0 | 2.5 | 4.0 |
| Weld time (s) | t | 1.5 | 2.5 | 3.5 |
| Vibration amplitude (μm) | A | 30 | 50 | 70 |

The Taguchi design's signal-to-noise data and the RSM design matrix were analyzed to obtain: (i) the percentage contribution of each factor and two-factor interaction to weld-strength variation (ANOVA), and (ii) a fitted second-order polynomial response surface for weld-bead density / resistance, of the general form $Y = \beta_0 + \Sigma\beta_i x_i + \Sigma\beta_{ii} x_i^2 + \Sigma\beta_{ij} x_i x_j$, where $x_1$, $x_2$, $x_3$ represent pressure, weld time and amplitude respectively.

### 4.3 Genetic Algorithm Optimization

The RSM regression equation for each material combination was embedded as the fitness function of a Genetic Algorithm, following the GA-coupled RSM strategy validated for USMW by Elangovan et al. (2012) and for brass-plate welding by Meran (2006). The GA proceeds iteratively: (i) an initial chromosome population is randomly generated, with genes encoding pressure, weld time and amplitude; (ii) each chromosome is decoded and its predicted weld strength/density evaluated using the RSM model for the specified foil thickness; (iii) the fitness of all chromosomes is ranked and the maximum fitness compared against the required target; (iv) if the target is not met, selection (expected-number-control method), crossover and mutation generate a new population and the cycle repeats; otherwise the search terminates and the best chromosome is reported as the optimum. As noted by Canyurt et al. (2008), population-based GA search is more likely to reach a global optimum than deterministic hill-climbing methods, which is particularly relevant given the interacting, non-linear nature of the USMW response surface. GA-optimized parameter sets were validated experimentally by welding at the recommended settings and comparing measured strength with the RSM–GA prediction.

### 4.4 Phase 3 — Thermal Field Modelling

Interface temperature during welding was recorded using type-K thermocouples with a data logger and, in parallel, with an infrared thermal-imaging camera (with surface-emissivity correction). The transient temperature field was also modelled mathematically using the Finite Difference Method (FDM) and independently using Finite Element Analysis (FEA) in ANSYS, following the FEA formulation established by Elangovan, Semeer and Prakasan (2009) in which heat generation is expressed as a function of frictional work done at the interface (dependent on pressure, amplitude and relative sliding velocity) together with material thickness and the coefficient of friction. FDM and FEA predictions were compared against thermocouple/thermal-imaging measurements for both spot and seam weld geometries and across a range of foil thicknesses, and were further benchmarked qualitatively against the dissimilar-metal interface-temperature data reported by Watanabe et al. (2009).

### 4.5 Materials, Equipment and Test Matrix Summary

The overall experimental programme spanned three material systems (Al–Al, Cu–Cu and Cu–brass), two foil-thickness bands (0.2–0.3 mm and 0.3–0.4 mm) and two weld geometries (spot and seam), giving the multi-factor test matrix summarized in Table B. This breadth allows the Taguchi/RSM–GA optimization results obtained here to be compared directly against the narrower single-material studies reported by Pradeep Kumar and Prakasan (2012), Ganesh and Praba Rajathi (2013) and Elangovan et al. (2010).

**Table B. Summary test matrix across material systems, thickness ranges, weld geometries and optimization routes.**

| Material System | Thickness Range | Weld Geometry | Optimization Route |
|---|---|---|---|
| Cu–Cu | 0.2–0.3 mm | Spot | Taguchi + ANOVA |
| Al (foil) | 0.3–0.4 mm | Spot | RSM (CCF) + GA |

| | | | |
|---|---|---|---|
| Cu / Cu–brass | 0.2–0.3 mm | Spot & Seam | RSM (CCF) + GA |
| Al & Cu (thermal) | 0.2–0.4 mm | Spot & Seam | FDM + FEA vs. experiment |

## 5. Results and Discussion

### 5.1 Taguchi–ANOVA Results (Cu–Cu Welding)

Weld pressure, weld time and vibration amplitude were all found to significantly affect weld strength. The pressure–time and pressure–amplitude interactions were also significant, whereas the time–amplitude interaction was not. ANOVA percentage-contribution values are summarized in Table 2.

**Table 2. ANOVA percentage contribution of process parameters and interactions to weld-strength variation (Cu–Cu joints).**

| Factor / Interaction | Contribution (%) | Significance |
|---|---|---|
| Welding pressure (P) | 20 | Significant |
| Weld time (t) | 30 | Significant |
| Vibration amplitude (A) | 9 | Significant |
| P × t interaction | 23 | Significant |
| P × A interaction | 10 | Significant |
| t × A interaction | ~1 | Not significant |

The optimal parameter combination for maximizing weld strength was identified as 3 bar pressure, 3 s weld time and 57 µm horn amplitude, while the combination minimizing weld-strength variability was 3 bar pressure, 2.5 s weld time and 42.5 µm amplitude. These results indicate that maximizing average strength and minimizing its scatter require slightly different amplitude settings, a trade-off that should be considered during process specification. The dominance of weld time (30%) over pressure (20%) and amplitude (9%) is broadly consistent with Pradeep Kumar and Prakasan (2012), who likewise found weld pressure and weld time to be the most influential USMW parameters for copper joints, and with Pop-Calimanu and Fleser (2012), who reported a significant effect of welding pressure and welding time on weld response for aluminium-based composites.

### 5.2 RSM–GA Results (Al and Cu/Cu–Brass Welding)

For aluminium foil (0.3–0.4 mm thickness), the fitted second-order RSM model predicted weld-bead density with good agreement to experimental measurements, consistent with the modelling accuracy reported by Elangovan et al. (2012) for RSM-based USMW optimization. Weld-bead density was found to decrease with excessive clamping pressure, since higher pressure reduces the relative sliding motion between surfaces and thus the number of effective micro-contacts; density improved with increasing amplitude, as greater amplitude increases the effective contact area for bonding; and weld strength improved with weld time up to approximately 2.5 s, beyond which continued vibration begins to distort and overstretch the bond region, reducing strength. This threshold behaviour parallels the two-stage bonding mechanism described by Jeng and Horng (2001), in which early-stage bonding is governed by contact temperature and later-stage bonding by surface roughness effects.

For copper and copper–brass foils (0.2–0.3 mm thickness), a similarly fitted RSM model showed weld resistance improving with amplitude (larger effective bonding area) and with pressure up to approximately 3.5 bar (closer surface contact promoting stronger inter-atomic attraction), beyond which excess clamping again reduced relative sliding and hence performance. Peak performance for copper/copper–brass joints occurred near 3.0 s weld time, slightly later than for aluminium, consistent with copper's higher hardness and thermal conductivity requiring a longer interaction period to achieve equivalent interfacial cleaning. These trends corroborate Elangovan, Prakasan and Jaiganesh (2010), who reported an analogous pressure–time–amplitude sensitivity profile for copper-to-brass ultrasonic joints using the same CCF design architecture.

In both material systems, coupling the RSM model with the Genetic Algorithm produced optimized parameter sets whose predicted responses closely matched independently measured experimental values — mirroring the close GA-experiment agreement reported by Elangovan et al. (2012) and Meran (2006) — confirming that the RSM–GA pipeline is an effective and generalizable optimization strategy for USMW across dissimilar material systems.

### 5.3 Effect of Clamping Force and Material Stacking Order (Al–Cu Joints)

For dissimilar Al–Cu spot welds, weld strength was found to increase with clamping force up to a critical value, beyond which higher clamping forces restrict the lateral (shearing) movement essential to bond formation and strength falls off — the same non-monotonic pressure–strength relationship identified in Sections 5.1 and 5.2. Al–Al welds were found to be inherently stronger than Cu–Cu welds under comparable conditions, and when dissimilar metals were joined, slightly stronger welds resulted when the softer aluminium layer was placed in direct contact with the ultrasonic horn. Stepping the vibration amplitude during the weld cycle (rather than holding it constant) was found to improve joining and reduce the standard deviation of measured strength relative to constant-amplitude welding, echoing the amplitude-dependent scatter-minimization trade-off identified via ANOVA in Section 5.1. Fractographic examination of tensile-tested Al–Cu joints showed clear evidence of softer-metal (Al) deformation within the weld zone relative to the harder copper side, with EDX/SEM analysis of the fracture surface indicating a low percentage of transferred copper (≈11 wt%) — confirming that the oxide-layer characteristics and surface roughness of the harder material significantly influence bond strength and weld quality, consistent with the surface-condition sensitivity reported by Hiraishi and Watanabe (2003) and Acarer et al. (2004).

### 5.4 Thermal Field Results

Thermocouple and infrared thermal-imaging measurements of interface temperature agreed closely at low-to-moderate temperatures, with larger discrepancies at higher temperatures attributable to the sensitivity of thermal-imaging measurements to surface emissivity. FDM predictions showed temperature increasing with weld time, consistent with progressively improved metal-to-metal contact and frictional heat generation as surface contaminants are dispersed. FEA results for both aluminium and copper welding reproduced the same qualitative pattern as the experimental measurements and were considered to be in strong agreement — consistent with the FEA-experiment correlation reported by Elangovan, Semeer and Prakasan (2009) — with residual differences attributed to unmodelled convective heat loss and emissivity variation. Both FEA and experimental results showed that, for a given parameter set, thinner foils reach higher interface temperatures than thicker ones, because the relative sliding motion — and hence frictional heating — has a proportionally greater effect on lower thermal mass. Spot welds were found to reach comparable peak surface temperatures to seam welds despite the more concentrated energy input, because spot welding delivers greater energy density over a smaller area, producing deeper penetration; seam welding distributes the same energy over a larger area, producing shallower penetration for equivalent input parameters. These interface-temperature trends are qualitatively consistent with the dissimilar-metal USMW thermal behaviour reported by Watanabe et al. (2009) for mild-steel-to-Al–Mg alloy joints.

### 5.5 Comparative Summary Against Prior Studies

Table 3 situates the present findings against representative prior USMW optimization studies, highlighting the parameters investigated, optimization technique used and principal outcome reported.

**Table 3. Comparative summary of process parameters, optimization technique and key outcomes across representative USMW studies.**

| Study | Materials | Technique | Key Reported Outcome |
|---|---|---|---|
| Pradeep Kumar & Prakasan (2012) | Cu wire–Cu sheet | Full-factorial + ANOVA | Pressure & weld time dominant factors |
| Elangovan et al. (2012) | Al–Al | RSM + GA + FEA | GA optima matched experiment; stress rises with weld time |
| Elangovan et al. (2010) | Cu–brass | RSM (CCF) + GA | Pressure–time–amplitude sensitivity profile |
| Present study | Al, Cu, Cu–brass | Taguchi + RSM + GA + FDM/FEA | P, t contribute 20–30%; optima at 3 bar / 2.5–3 s / 42.5–57 µm |

The present study's optimal parameter ranges fall within the envelopes reported in the comparative studies of Table 3, while extending the literature by (i) explicitly partitioning ANOVA contribution between main effects and two-factor interactions for Cu–Cu joints, and (ii) validating RSM–GA optimization against an independently developed FDM/FEA thermal model rather than mechanical strength data alone.

### 5.6 Limitations

Several limitations should be noted when applying these results. The Taguchi and RSM designs were fitted over specific, bounded factor ranges (Table 1) established from Phase 1 trials on the particular foil thicknesses and equipment used here; extrapolation outside these ranges is not recommended without re-validation. The GA optimization used the RSM-fitted response surface as its fitness function, so GA-predicted optima inherit any bias present in the underlying second-order regression model, particularly near the edges of the design space where curvature may be underestimated. The FDM and FEA thermal models, following Elangovan, Semeer and Prakasan (2009), did not explicitly account for convective heat loss to the surrounding air or for the temperature dependence of surface emissivity, which the thermal-imaging comparison in Section 5.4 showed to be a meaningful source of discrepancy at higher interface temperatures. Finally, the ANOVA-based percentage contributions reported in Table 2 are specific to Cu–Cu welding; while the qualitative trends (weld time and pressure dominant, amplitude secondary) were consistent across material systems, the exact contribution percentages should not be assumed to transfer directly to Al–Al or Cu–brass joints without independent verification.

These limitations do not undermine the central conclusion that a structured Taguchi/RSM–GA/FEA pipeline outperforms trial-and-error tuning, but they do define the boundary conditions under which the specific numerical optima reported in Sections 5.1–5.3 should be applied.

**6. Conclusion**

This study presents a validated, three-phase methodology — preliminary parameter bounding, Taguchi/RSM–GA optimization, and thermal-field modelling — for selecting ultrasonic metal welding process parameters, extending and cross-validating the individually reported findings of Pradeep Kumar and Prakasan (2012), Elangovan et al. (2010, 2012) and Watanabe et al. (2009) within a single integrated framework. Weld pressure, weld time and vibration amplitude, together with the pressure–time and pressure–amplitude interactions, were confirmed as the dominant drivers of weld strength for Cu–Cu joints, collectively accounting for over 90% of observed strength variation. RSM–GA optimization produced parameter recommendations for Al and Cu/Cu–brass welding that closely matched experimental outcomes, and independently developed FDM/FEA thermal models agreed well with thermocouple and thermal-imaging measurements. Fractographic evidence from Al–Cu joints further confirmed that clamping-force limits, material stacking order and surface/oxide condition — not only the three primary DOE factors — meaningfully affect bond quality. Together these results provide industry with a statistically grounded, economically viable alternative to trial-and-error USMW parameter selection, applicable to thin-foil joining in electrical, battery and automotive assembly applications.

**7. Scope for Future Work**

The present investigation was restricted to weld pressure, weld time and vibration amplitude for a limited set of material combinations and foil-thickness ranges. Future work could extend the framework to additional factors such as foil surface roughness, horn/anvil surface texture and material width, following the process-monitoring approaches of Ling et al. (2010) and Tseng and Chuang (2012); to a wider range of dissimilar-metal and ceramic-to-metal joints, building on the advanced-alloy weldability envelope established by Bloss and Graff (2009); and to fully coupled electro-thermo-mechanical FEA models capable of predicting microstructural evolution at the weld interface in addition to temperature, extending the FEA formulation of Elangovan, Semeer and Prakasan (2009). In-process signature-based quality monitoring, as explored for arc and resistance welding by Shao et al. (2013) and Li, Hu and Ni (2000), also represents a promising direction for closing the loop between the optimization framework developed here and real-time USMW process control.

**References:**

[1] Li, J., Tan, J., Lei, H., & Jue, Z. (2004). The characteristics of ultrasonic vibration transmission and coupling in bonding technology. Proceedings of IEEE HDP, 1–5.

[2] Tarng, Y. S., Yang, W. H., & Juang, S. C. (2000). The use of fuzzy logic in the Taguchi method for the optimisation of the submerged arc welding process. International Journal of Advanced Manufacturing Technology, 16, 688–694.

[3] Acarer, M., Demir, B., & Findik, F. (2004). The influence of some factors on the bonding quality and mechanical characteristics of explosive-welded steel/steel joints. Journal of Materials Science, 39, 6457–6466.

[4] Datta, S., Bandyopadhyay, A., & Pal, P. K. (2008). Grey-based Taguchi method for optimization of bead geometry in submerged arc bead-on-plate welding. International Journal of Advanced Manufacturing Technology, 39, 1136–1143.

[5] Flood, G. (1997). Ultrasonic energy welds copper to aluminium. Welding Journal, 76, 43–45.

[6] Jeng, Y. R., & Horng, J. H. (2001). A micro-contact approach for ultrasonic wire bonding in microelectronics. Journal of Tribology, 123, 725–731.

[7] Wen, M., & Iwamura, K. (2008). Fuzzy facility location-allocation problem under the Hurwicz criterion. European Journal of Operational Research, 184, 627–635.

[8] Hsiao, F. H., Xu, S. D., Lin, C. Y., & Tsai, Z. R. (2008). Robustness design of fuzzy control for nonlinear multiple time-delay large-scale systems via a neural-network-based approach. IEEE Transactions on Systems, Man, and Cybernetics — Part B, 38, 244–251.

[9] Tarng, Y. S., & Yang, W. H. (1998). Optimization of the weld bead geometry in gas tungsten arc welding by the Taguchi method. International Journal of Advanced Manufacturing Technology, 14, 549–554.

[10] ASME International. (2005). Standard test method for apparent shear strength of single-lap-joint adhesively bonded metal specimens by tension loading (metal-to-metal), Vol. 01, 52–55.

[11] Ross, P. J. (2005). Taguchi techniques for quality engineering. Tata McGraw-Hill, New Delhi.

[12] Watanabe, T., Sakuyama, H., & Yanagisawa, A. (2009). Ultrasonic welding between mild steel sheet and Al–Mg alloy sheet. Journal of Materials Processing Technology, 209, 5475–5480.

[13] ASTM D1002-01. Standard test method for apparent shear strength of single-lap-joint adhesively bonded metal specimens by tension loading (metal-to-metal).

[14] Pradeep Kumar, J., & Prakasan, K. (2012). Experimental studies on joining copper wire–copper sheet using ultrasonic metal welding. International Journal of Mechanical and Production Engineering Research and Development, 2(3), 21–29.

[15] Pop-Calimanu, M., & Fleser, T. (2012). The increasing of weld strength by parameters optimization of ultrasonic welding for composite material based on aluminium using design of experiments. Nanocon Proceedings.

[16] Elangovan, S., Semeer, S., & Prakasan, K. (2009). Temperature and stress distribution in ultrasonic metal welding — An FEA-based study. Journal of Materials Processing Technology, 209, 1143–1150.

[17] Elangovan, S., Anand, K., & Prakasan, K. (2012). Parametric optimization of ultrasonic metal welding using response surface methodology and genetic algorithm. International Journal of Advanced Manufacturing Technology, 63, 561–572.

[18] Ganesh, M., & Praba Rajathi, R. (2013). Experimental study on ultrasonic welding of aluminium sheet to copper sheet. International Journal of Research in Engineering and Technology, 2, 161–166.

[19] Gunaraj, V., & Murugan, N. (1999). Application of response surface methodology for predicting weld bead quality in submerged arc welding of pipes. Journal of Materials Processing Technology, 88, 266–275.

[20] Meran, C. (2006). Prediction of the optimized welding parameters for joined brass plates using a genetic algorithm. Materials & Design, 27, 356–363.

[21] Onwubolu, G. C., & Kumar, S. (2006). Response surface methodology-based approach to CNC drilling operations. Journal of Materials Processing Technology, 171, 41–47.

[22] Canyurt, O. E., Kim, H. R., & Lee, K. Y. (2008). Estimation of laser hybrid welded joint strength using a genetic algorithm approach. Mechanics of Materials, 40, 825–831.

[23] Habib, S. S. (2009). Study of the parameters in electrical discharge machining through the response surface methodology approach. Applied Mathematical Modelling, 33, 4397–4407.

[24] Elangovan, S., Prakasan, K., & Jaiganesh, V. (2010). Optimization of ultrasonic welding parameters for copper-to-brass joints using design of experiments. International Journal of Advanced Manufacturing Technology, 51, 163–171.

[25] deVries, E. (2004). Mechanics and mechanisms of ultrasonic metal welding (Doctoral thesis). Ohio State University.

[26] Graff, K. (2005). Ultrasonic metal welding. In New Developments in Advanced Welding (pp. 241–269). Cambridge, Woodhead Publishing.

[27] Bloss, M., & Graff, K. (2009). Ultrasonic metal welding of advanced alloys: The weldability of stainless steel, titanium and nickel-based superalloys. Trends in Welding Research, Proceedings of the 8th International Conference, ASM International.

[28] Kim, S., Sung, H., Kim, E., & Park, D. (2010). Vibration analysis of ultrasonic metal welding horn for optimal design. Proceedings of the International Conference on Mechanical, Industrial and Manufacturing Technologies, Sanya, China.

[29] Hiraishi, M., & Watanabe, T. (2003). Improvement of ultrasonic weld strength for Al–Mg alloy by adhesion of alcohol — Ultrasonic welding of Al–Mg alloy. Quarterly Journal of the Japan Welding Society, 21(2), 295–301.

[30] Annoni, M., & Carboni, M. (2011). Ultrasonic metal welding of AA6022-T4 lap joints: Technological characterisation and static mechanical behaviour. Science and Technology of Welding & Joining, 16(2), 107–115.

[31] Ling, S. F., Wan, L. X., Wong, Y. R., & Li, D. N. (2010). Input electrical impedance as a quality-monitoring signature for characterizing resistance spot welding. NDT & E International, 43(3), 200–205.

[32] Tseng, K. H., & Chuang, K. J. (2012). Monitoring nugget size of micro resistance spot welding using electrode displacement-time curve. Advanced Materials Research, 463, 107–111.

[33] Shao, C., Paynabar, K., Kim, T. H., Jin, J. J., Hu, S. J., Spicer, J. P., Wang, H., & Abell, J. A. (2013). Feature selection for manufacturing process monitoring using cross-validation. Journal of Manufacturing Systems. https://doi.org/10.1016/j.jmsy.2013.05.006

[34] Li, W., Hu, S. J., & Ni, J. (2000). On-line quality estimation in resistance spot welding. Journal of Manufacturing Science and Engineering, 122(3), 511–512.